Structure of the regulatory subunit of CK2 in the presence of a p21^{WAF1} peptide demonstrates flexibility of the acidic loop

Loic Bertrand,[a]‡§ Muhammed F. R. Sayed,[a]‡¶ Xue-Yuan Pei,[a] Emilio Parisini,[a]‡‡ Venugopal Dhanaraj,[a] Victor M. Bolanos-Garcia,[a] Jorge E. Allende[b] and Tom L. Blundell[a]*

[a]Department of Biochemistry, University of Cambridge, 80 Tennis Court Road, Cambridge CB2 1GA, England, and [b]Programa de Biología Celular y Molecular, ICBM, Facultad de Medicina, Universidad de Chile, Independencia 1027, Santiago, Chile

‡ The two first authors contributed equally to this paper.
§ Current affiliation: Laboratoire de Physique des Solides, Université Paris-Sud, Bâtiment 510, 91405 Orsay CEDEX, France.
¶ Current affiliation: Department of Biotechnology, University of the Western Cape, Bellville 7535, Republic of South Africa.
‡‡ Current affiliation: Dana-Farber Cancer Institute, Harvard Medical School, 44 Binney Street, Boston MA 02115, USA.

Correspondence e-mail: tom@cryst.bioc.cam.ac.uk

A truncated form of the regulatory subunit of the protein kinase CK2β (residues 1–178) has been crystallized in the presence of a fragment of the cyclin-dependent kinase inhibitor p21^{WAF1} (residues 46–65) and the structure solved at 2.9 Å resolution by molecular replacement. The core of the CK2β dimer shows a high structural similarity with that identified in previous structural analyses of the dimer and the holoenzyme. However, the electron density corresponding to the substrate-binding acidic loop (residues 55–64) indicates two conformations that differ from that of the holoenzyme structure [Niefind *et al.* (2001), *EMBO J.* **20**, 5320–5331]. Difference electron density near the dimerization region in each of the eight protomers in the asymmetric unit is attributed to between one and eight amino-acid residues of a complexed fragment of p21^{WAF1}. This binding site corresponds to the solvent-accessible part of the conserved zinc-finger motif.

PDB Reference: CK2β–p21^{WAF}, 1rqf, r1rqfsf.

This article was written in memory of Venugopal Dhanaraj.

1. Introduction

Protein kinase CK2 is a ubiquitous serine/threonine kinase in eukaryotes that is known to phosphorylate more than 300 cellular proteins (Allende & Allende, 1995; Meggio & Pinna, 2003). These range from transcription factors to proteins participating in cell signalling to those involved in chromatin structure. Numerous findings suggest a role for CK2 in the control of cell division, differentiation and virus infection (Pinna & Meggio, 1997; Guerra & Issinger, 1999). Native CK2 forms heterotetrameric complexes consisting of two catalytic (α or α') and two regulatory (β) subunits. The detailed structural mechanism of the regulation by the β subunit of the phosphorylating activity of the catalytic subunit is not well understood, although the structures of the two separate subunits and the holoenzyme have recently been solved (Niefind *et al.*, 1998, 2001; Chantalat *et al.*, 1999). It is clear, however, that the function of the regulatory β subunit is not merely one of activating the catalysis in the α-subunit, since with several substrates the regulatory subunit has been shown to be inhibitory rather than stimulatory.

An interesting feature is the presence of a highly conserved zinc-finger domain mediating the dimerization of the CK2β subunits. The dimer has a crescent shape with a region of acidic amino acids at each extremity resulting from an acidic loop (Asp55–Asp64), which forms part of an an extended acidic groove and plays an important role in the modulation of CK2 activity (Boldyreff *et al.*, 1993, 1994*b*). It has also been postulated that this acidic stretch encompassing residues 55–64 of CK2β interacts with a basic cluster of amino acids on the catalytic subunit of CK2 (*i.e.* residues 74–80 of CK2α) within the same tetrameric CK2 complex. However, the structure of

tetrameric CK2 shows that this acidic stretch is far away from the active site of the catalytic subunit.

The regulatory β subunit has been found to bind several proteins that are substrates of CK2, a large proportion of which are important regulators of cell division, such as p53 (Appel *et al.*, 1995) and $p21^{WAF1}$ (Appel *et al.*, 1995; Götz *et al.*, 1996, 2000; Romero-Oliva & Allende, 2001). Recently, we have also shown that CK2β binds to the cyclin-dependent kinase (CDK) complex inhibitor $p27^{KIP1}$ (Tapia *et al.*, 2004). Such binding *via* the β subunit is consistent with a contribution of the kinase regulatory subunits to the affinity and selectivity of the enzyme for various substrates by providing docking sites (Holland & Cooper, 1999), thus increasing the effective substrate concentration in the vicinity of the catalytic active site.

In order to gain further insight into the structural features of the CK2β docking site, we crystallized CK2β in the presence of a fragment of $p21^{WAF1}$. $p21^{WAF1}$, a universal inhibitor of cyclin-dependent kinases, regulates cell division by forming distinct protein complexes with cyclins, CDKs and the proliferating cell nuclear antigen. Previous studies have demonstrated that a region of $p21^{WAF1}$ essential for kinase inhibition, encompassing residues 46–65, binds to CK2 (Götz *et al.*, 1998).

The $p21^{WAF1}$-binding region on the CK2β subunit has been a source of controversy. Far-Western assays implicate three regions: an N-terminal region (residues 9–31), an intermediate region (residues 49–63), which encompasses the acidic loop, and the C-terminal (201–215) region of CK2β (Götz *et al.*, 2000). However, recent pull-down experiments do not support binding to the acidic loop or the C-terminus of CK2, but underline the importance of the N-terminal region 1–44 (Romero-Oliva & Allende, 2001). Both studies were carried out using full-length $p21^{WAF1}$. Moreover, the medium region 71–150 of CK2β was not reported to bind wild-type $p21^{WAF1}$ (Götz *et al.*, 2000). It has also been suggested that the solvent-accessible region in the zinc-finger motif may be important for binding substrates (Chantalat *et al.*, 1999).

In this work, we use a C-terminal truncated form of the CK2β subunit, residues 1–178, for crystallization in the presence of a fragment of $p21^{WAF1}$, residues 46–65. We report two new conformations of the substrate-binding acidic loop that differ from that in the holoenzyme structure. Our study suggests that the binding site of $p21^{WAF1}$ to $CK2\beta^{1-178}$ corresponds to the solvent-accessible part of the conserved zinc-finger motif. $p21^{WAF1}$ is likely to adopt a non-globular conformation to bind CK2.

2. Materials and methods

2.1. Protein purification

The gene encoding $CK2\beta^{1-178}$ from *Xenopus laevis* (100% sequence identical to the human) was fused to the glutathione *S*-transferase gene by cloning into the vector pGEX-2T (Amersham) at the *Eco*RI restriction site for both 5′ and 3′ extremities (Hinrichs *et al.*, 1995). The resulting recombinant vector was transformed into *Escherichia coli* strain BL21(DE3) (Amersham). After induction with IPTG at a final concentration of 0.1 m*M* and growth for 3 h at 310 K, the cells were harvested. The bacterial pellet was resuspended in lysis buffer (buffer *A*: 50 m*M* Tris–HCl, 200 m*M* NaCl, 1 m*M* DTT pH 8.0 containing a cocktail of protease inhibitors). After sonication, particulate material was removed by centrifugation at 15 000*g* for 30 min. The supernatant was loaded onto a Glutathione Sepharose 4B syringe column (Amersham). The column was washed with buffer *A* and the fusion protein eluted with the same buffer containing 20 m*M* reduced glutathione. All protein-containing fractions were concentrated with a Centricon concentrator (Amicon; 30 kDa molecular-weight cutoff membrane) and incubated at 277 K overnight with 1 unit of thrombin per milligram of fusion protein. The completeness of digestion of the fusion protein was monitored by SDS–PAGE. The cleavage leaves six additional residues at the N-terminal extremity of CK2β, as confirmed by N-terminal sequencing. After cleavage, the protein solution was pumped through the glutathione Sepharose 4B column to remove the GST fragment. The $CK2\beta^{1-178}$ protein was loaded onto a Resource Q ion-exchange column (Amersham) and eluted using a linear gradient from 0.2 to 1 *M* NaCl. Samples were further purified by gel filtration (Superdex 200 HR 10/30 column; equilibrated and eluted with buffer *A*). Gel-filtration experiments confirmed that the protein forms a dimer in solution. The purified protein was concentrated to 15–20 mg ml^{-1} using a Centricon (10 kDa cutoff).

A peptide containing residues 46–65 of $p21^{WAF1}$ was synthesized using a Pioneer peptide synthesiser (Applied Biosystems). The peptide identities were corroborated by laser-desorption mass spectrometry and HPLC analysis.

A twofold molar excess of $p21^{WAF1}$ was added to a concentrated sample of purified $CK2\beta^{1-178}$, usually at 20 mg ml^{-1}. The mixture was left to equilibrate overnight at 277 K before setting up any crystallization screens. The hanging-drop vapour-diffusion method was used to screen crystallization conditions. The first crystals were obtained in a solution containing 20% PEG 4000 and 20% 2-propanol from a sparse-matrix kit (Hampton Research). Plate-like crystals formed after 2 d equilibration at room temperature against a well solution of 20% polyethylene glycol 4000 (PEG 4000) in Bicine buffer pH 9.2, 30 m*M* $MgCl_2$, 1 m*M* DTT and 5% 2-propanol. Drops using the same conditions, without addition of the $p21^{WAF1}$ peptide, were set up for comparison.

2.2. Crystal characterization

Several large crystals were harvested from their crystallization drops and washed in a 10–20 µl drop of stabilizing solution. The stabilizing solution typically contained 5% more precipitant agent than the reservoir solution of the corresponding crystallization condition. After 2–4 min, the crystals were transferred again into a fresh drop of stabilizing solution. The procedure was repeated four to five times to ensure that no layer of the original protein solution was still present on the

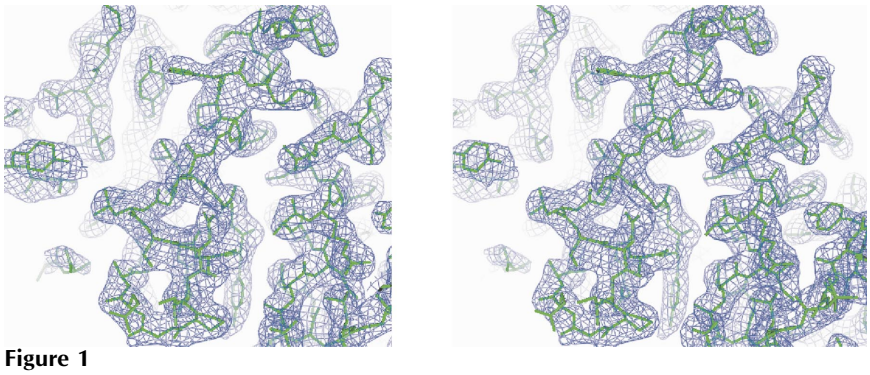

Figure 1
Stereoview of the refined model and $2F_o - F_c$ electron-density map in a part of the core region of CK2β. The electron-density map is contoured at 1.0σ above the mean density. Figs. 1, 2, 4, 5 and 7 were drawn using *PyMOL* (DeLano, 2002).

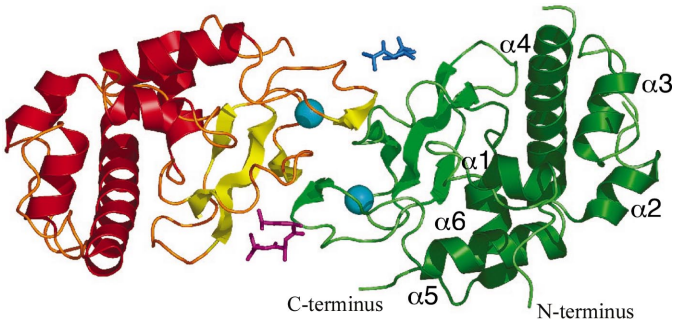

Figure 2
Ribbon representation of the CK2β^{1-178} dimer structure. The blue and purple residues correspond to the polyalanine model. The Zn atoms are represented by blue spheres.

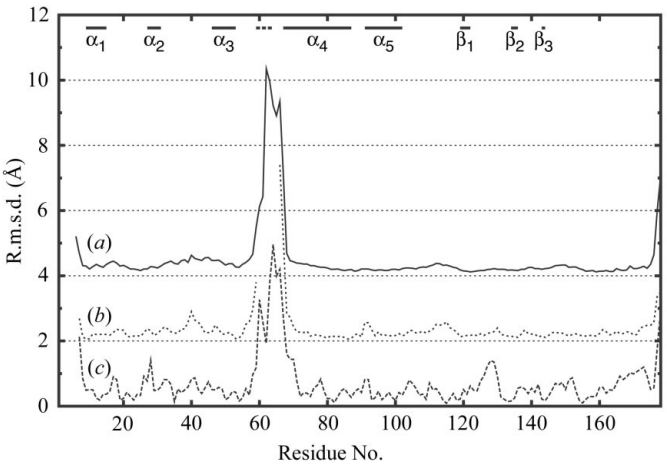

Figure 3
Root-mean-square variation in distance among the eight NCS-related protomers in the CK2β^{1-178} structure (*a*), between the chain *A* and chains from 1qf8 (*b*) and between the chain *A* and chains from 1jwh (*c*). Calculations were made using *LSQMAN* (Kleywegt, 1996). Graphs are shifted from the origin for clarity.

surface of the crystal. The crystals were then dissolved in water for MALDI–TOF analysis and in 5 µl loading buffer for SDS–PAGE analysis.

2.3. X-ray data collection

The crystals were soaked for several minutes in a cryoprotecting solution containing 20% PEG 4000, 5% 2-propanol, 400 m*M* NaCl, 30 m*M* $MgCl_2$, 50 m*M* Bicine pH 9.2 and 20% glycerol. The diffraction data were collected from a single crystal at 100 K to 2.9 Å resolution at synchrotron beamline ID14-1 (ESRF, Grenoble). The X-ray data were processed using the program *MOSFLM* (Leslie, 1992) and scaled and reduced using programs from the *CCP*4 suite (Collaborative Computational Project, Number 4, 1994).

Small-angle X-ray scattering (SAXS) data were collected at station 2.1 at the SRS (Daresbury, UK). CK2β^{1-178} solutions in 50 m*M* Tris–HCl buffer pH 8.0 were analysed at 293 K. Distance-distribution functions $\rho(r)$ and the radius of gyration R_g were evaluated with the indirect Fourier transform using the program *GNOM* (Svergun, 1991).

2.4. Structure determination, model building and refinement

The crystal structure was determined by molecular replacement using that of CK2β as a search probe (PDB code 1qf8; Chantalat *et al.*, 1999), with *MOLREP* performing rotation and translation searches. An initial correlation coefficient of 58.3% was obtained. The refinement was performed using *REFMAC*5, first through restrained refinement and subsequently by defining TLS groups corresponding to each protomer. Further steps of refinement were performed with *CNS* energy minimization and *B*-factor refinement using bulk-solvent correction. Tight NCS restraints for atomic coordinates and *B* factors were applied to main-chain and side-chain atoms. Atoms from the N- and C-termini, as well as the acidic loop, were excluded from these restraints. Torsion simulated annealing was performed and an $(F_o - F_c)$ difference map generated to assess the presence of the peptide using *CNS sa_omit_map* (starting temperature, 4000 K; drop, 25 K per set; Brünger *et al.*, 1998).

3. Results

3.1. Overall structure analysis

Analysis of the plate-like crystals by SDS–PAGE confirmed the presence of CK2β^{1-178}. The space group, $P2_12_12$, of the crystals of CK2β^{1-178} differs from that of the previous structure of the CK2β subunit ($P4_12_12$; Chantalat *et al.*, 1999). The structure was solved at a resolution of 2.9 Å and refined to a crystallographic *R* factor of 23.8% and R_{free} of 26.6% (see Table 1). The quality of the map allowed rebuilding of the main part of the core regions (Fig. 1). The overall tertiary structure of CK2β^{1-178} shows the expected crescent-shaped CK2β dimer (Fig. 2).

The CK2β protomer consists of two tightly packed domains. Domain I is predominantly helical in nature and forms a characteristic L-shape as observed in the previous CK2 dimer structure. Domain II consists of a three-stranded antiparallel β-sheet with four conserved cysteines (109, 114, 137 and 140)

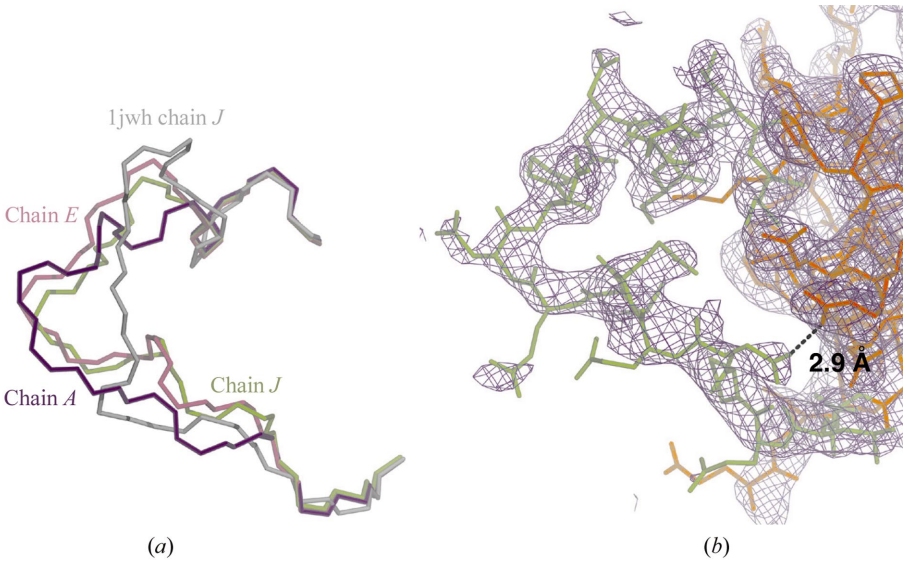

Figure 4
(*a*) Comparison showing the different conformations of the acidic loop backbone (region 55–72): chain *A* (blue), chain *E* (magenta) and the similar chain *J* (green) from the present CK2β^{1-178} structure and chain *D* from the holoenzyme structure (grey, PDB code 1jwh; Chantalat *et al.*, 1999). (*b*) Part of the acidic loop backbone in chain *J* within the $2F_o - F_c$ electron-density map contoured at 1.0σ above the mean density. The salt bridge between Asp59 and Arg47 is indicated in black.

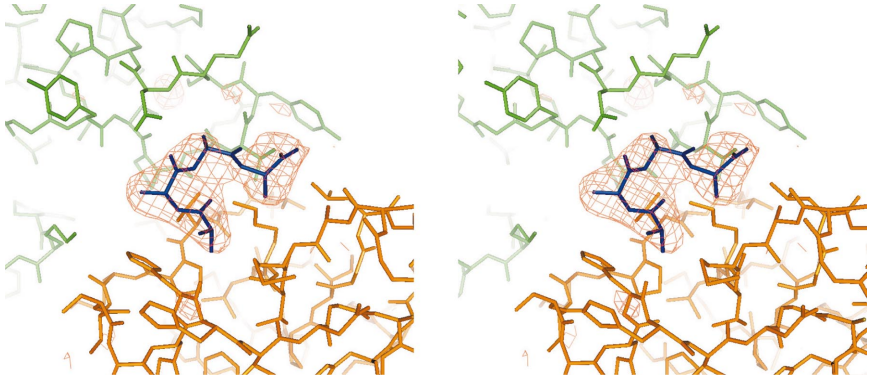

Figure 5
Stereoview of a peptide polyalanine model in the omit $F_o - F_c$ electron-density map. Residues from the peptide are printed in blue and contact the dimerization interface of the CK2β^{1-178} dimer formed by the *J* (orange) and *K* (green) protomers. The difference electron-density map is contoured at 3.0σ above the mean density.

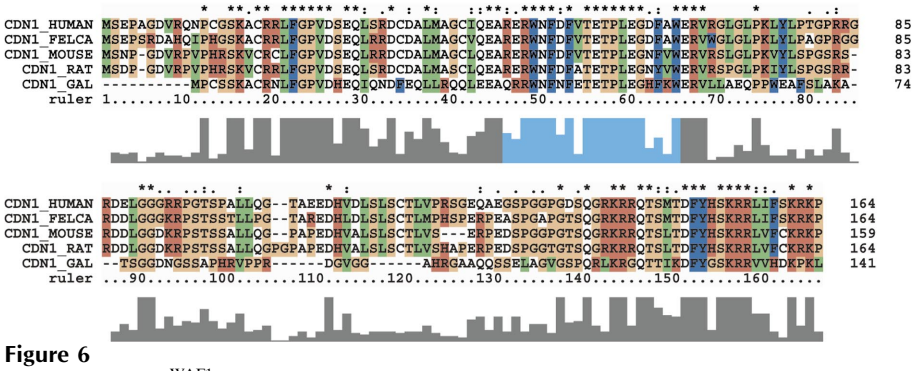

Figure 6
Alignment of p21^{WAF1} sequences from *Homo sapiens*, *Felis silvestris catus*, *Mus musculus*, *Rattus norvegicus* and *Gallus gallus*. The region corresponding to residues 46–65 of p21^{WAF1} is indicated in blue. The alignment was produced using *CLUSTALW* (Thompson *et al.*, 1997).

forming a Zn^{2+}-binding motif. However, the characteristic α-helix of classical zinc fingers is not present in this motif. The CK2 zinc motif is remarkably similar to the Zn^{2+}-ribbon of transcriptional elongation factor TFIIS, as reported earlier (Qian *et al.*, 1993; Chantalat *et al.*, 1999).

The above-mentioned acidic loop is located at the remote extremities of the dimer. Some residues in the termini and acidic loop regions could not be fitted into the electron density of some of the protomers and may be disordered, as observed in earlier structures of CK2 (see list of residues in Table 2). As shown in Table 2, our overall structure is very similar to that of the CK2β dimer (Chantalat *et al.*, 1999) and of the holoenzyme (PDB code 1jwh; Niefind *et al.*, 2001), indicating the absence of major reorganization of the β subunit in the presence of p21$^{WAF1,\ 46-65}$.

SAXS experiments were performed on CK2β^{1-178} at concentrations ranging from 1 to 10 mg ml^{-1} (~50–500 μM). CK2β^{1-178} showed an estimated gyration radius (R_g) of 27.5 Å. This result demonstrates that within this concentration range CK2β^{1-178} forms monodisperse dimers and no higher aggregates in aqueous solution. The overall shape of the electron density observed in solution is in good agreement with that determined from the X-ray structures.

3.2. Acidic loop

The most significant differences between the CK2β^{1-178} structure and that of the holoenzyme (PDB code 1jwh; Niefind *et al.*, 2001) arise in the acidic loop, residues 55–64 (Fig. 3). This region was suggested as a potential binding site for p21^{WAF1} and other substrates (Meggio *et al.*, 1994; Chen *et al.*, 1996; Leroy, Filhol *et al.*, 1997; Leroy, Heriche *et al.*, 1997; Götz *et al.*, 2000; Romero-Oliva & Allende, 2001). This acidic loop was not visible in the electron-density maps of the earlier CK2β dimer structure (Chantalat *et al.*, 1999), suggesting that this region adopts more than one conformation.

The present crystal structure of CK2β^{1-178} shows the main-chain back-

Table 1
X-ray diffraction data and refinement statistics for CK2β^{1-178}.

Values in parentheses are for the highest resolution shell. Ramachandran statistics were calculated using *PROCHECK* and mean *B* factors using *BAVERAGE* (Collaborative Computational Project, Number 4, 1994).

Crystal data	
Space group	$P2_12_12$
Unit-cell parameters (Å)	a = 145.42, b = 170.63, c = 74.55
Content of asymmetric unit	8 protomers of CK2β^{1-178}
Data statistics	
Resolution limits (Å)	12.00–2.89
No. of observations	
Included	397993
Unique	41256 (6741)
Independent, in working set (95%)	41064 (6429)
Independent, in free set (5%)	2048 (312)
Completeness (%)	99.5 (99.7)
R_{merge} (%)	6.7 (33.6)
Average $I/\sigma(I)$	7.2 (2.2)
Refinement and model statistics	
Resolution range in refinement (Å)	11.97–2.89 (3.08–2.89)
R_{work} (95% of all reflections) (%)	23.8 (36.2)
R_{free} (5% of all reflections) (%)	26.6 (37.1)
Mean B factor (Å^2)	80.4
For main-chain atoms	78.1
For side-chain atoms and waters	82.6
No. solvent molecules	65
Root-mean-square deviations	
For bond lengths (Å)	0.007
For bond angles (°)	1.2
Quality of Ramachandran plot	
Residues in most favoured regions (%)	90.7
Residues in additional allowed regions (%)	8.3
Residues in generously allowed regions (%)	1.0
Residues in disallowed regions (%)	0.0

bone of the acidic loop to be clearly defined in three of the eight protomers in the asymmetric unit (Fig. 4*b*). Moreover, two different conformations (1 and 2) are observed within these three protomers, diverging from Pro58 to Gln68 (Fig. 4*a*).

In two of the protomers (chain *E* and *J*), the acidic loop folds into a compact conformation (conformation 1; Fig. 4*a*), which differs from that reported in the holoenzyme structure. In conformation 1, the α4 α-helix is followed by a turn in residues Asp59–Asp64, as defined by *DSSP* (Kabsch & Sander, 1983). In the third protomer (chain *A*), the loop adopts conformation 2, diverging from residues 61–67. The loop is presumed to be disordered in the other protomers.

The rest of the molecule shows great similarity: the maximum r.m.s.d. between the main-chain atoms of two NCS-related protomers excluding the loop is 0.29 Å.

3.3. Ligand binding

The presence of p21^{WAF1} in the crystal structure was confirmed from the MALDI–TOF spectrum of dissolved crystals and the fact that no crystal could be grown in the absence of p21^{WAF1} using identical crystallization conditions.

No remaining significant positive peaks could be seen in the difference map around those regions where the acidic loop could be traced. It is therefore improbable that the fragment 46–65 of p21^{WAF1} binds to this region of CK2β.

Table 2
Minimal r.m.s.d.s (Å) between the eight non-crystallographically related protomers of the asymmetric unit and those from previous CK2β and holoenzyme structures, calculated with *LSQMAN* (Kleywegt, 1996).

The values in parentheses are the number of main-chain atoms taken into account in the calculation. Atoms from the acidic loop region, residues 58–68, have been excluded from the calculation.

Chain	Refined regions	1qf8, *A*	1qf8, *B*	1jwh, *C*	1jwh, *D*
A	7–178	0.348 (483)	0.318 (477)	0.720 (483)	0.732 (483)
B	6–58, 67–178	0.395 (483)	0.309 (480)	0.651 (486)	0.672 (486)
D	6–58, 66–177	0.398 (480)	0.383 (480)	0.720 (483)	0.725 (483)
E	6–178	0.384 (483)	0.349 (480)	0.779 (486)	0.778 (486)
G	5–58, 68–178	0.400 (483)	0.339 (480)	0.756 (486)	0.873 (489)
H	7–58, 66–178	0.490 (483)	0.326 (477)	0.670 (483)	0.683 (483)
J	6–178	0.387 (483)	0.345 (480)	0.762 (486)	0.803 (486)
K	2–58, 67–178	0.453 (483)	0.384 (480)	0.798 (486)	1.110 (498)

Continuous electron density could be seen near to the dimerization region of CK2β. The electron density still appears at the 3.0σ contour level in the omit map generated after simulated annealing using *CNS* (Fig. 5). This density allowed us to fit a polyalanine backbone of one to eight residues within the eight protomers of the asymmetric unit. It is improbable that this electron density corresponds to a disordered portion of the N- or C-terminus, as the distances are large.

On the CK2β side, the contact region includes residues Tyr113 and Glu115 from one protomer and Leu124, Glu130, Ala131, Lys134, Thr145 and His152 from the other. This region corresponds to the solvent-accessible part of the highly conserved zinc-finger motif and is therefore consistent with the observation of Chantalat *et al.* (1999) that some of the exposed and conserved segments (including Gly123–Ile127) of the zinc-finger motif were accessible for interactions with other molecules.

On the p21^{WAF1} side, the CK2β^{1-178} structure is consistent with the identification by Götz *et al.* (1998) of a binding site for p21^{WAF1} somewhere in the 46–65 region of the peptide. Moreover, alignment of the available sequences of p21^{WAF1} shows that this stretch of amino acids is highly conserved, particularly in the 48–61 region (Fig. 6).

3.4. Conclusions

This new crystal form confirms the great flexibility of the acidic activation loop of the regulatory subunit CK2β. However, the acidic loop still lies far away from the active site of CK2 catalytic subunit, as observed by Niefind *et al.* (2001). The superimposition of CK2α according to the holoenzyme structure indicates a distance exceeding 30 Å in the most favourable conformation. This separation contrasts with the observation that the acidic loop influences the intramolecular autophosphorylation of Ser2 of CK2β (Boldyreff *et al.*, 1994*a*), unless (i) the great flexibility of the activation loop enables it to adopt a conformation in which it binds the N-terminal region (Niefind *et al.*, 2001) and/or (ii) this 'auto'-phosphorylation mechanism results from the formation of higher order CK2 holoenzyme structures (Glover, 1986; Valero *et al.*, 1995; Rekha & Srinivasan, 2003; Litchfield, 2003). Interestingly, the

crystal packing of the CK2 holoenzyme in the 1jwh structure (Niefind *et al.*, 2001) gives clues about the nature of such a higher order assembly; the active site of a symmetrically related CK2α molecule is intercalated between the N-terminal and the activation loop of CK2β.

The putative binding region for p21^{WAF1} is similar to that implicated in related CDK inhibitors of CK2 regulatory subunit, as region 72–149 of CK2β has been suggested to interact with p53 (Appel *et al.*, 1995). This comparison is particularly striking as p53 was shown to compete with p21 binding and probably shares a common binding site (Götz *et al.*, 1996). Recent results suggest that p21^{WAF1} competition with other substrates may indeed be the main inhibitory mechanism of CK2 activity (Romero-Oliva & Allende, 2001).

Moreover, this binding site supports the hypothesis that p21^{WAF1} may adopt an extended non-globular conformation when binding to the CK2 holoenzyme for the following reasons.

(i) The cyclin-dependent kinase inhibitor p27^{KIP1}, which shows a high sequence similarity to p21^{WAF1} (sequence identity = 39.7% and E value = 3.1×10^{-7} according to *FASTA*3; Pearson & Lipman, 1988) is mainly unfolded in aqueous solution and adopts a non-globular conformation in a ternary complex with CDK2/cyclin A (Russo *et al.*, 1996; Flaugh & Lumb, 2001). Ongoing SAXS experiments show that in binding CK2β, p27^{KIP1} might retain a primarily non-globular conformation (unpublished results). The sequence similarity between p21^{WAF1} and p27^{KIP1}, as well as secondary-structure prediction using *PHD* (Rost & Sander, 1993), suggest that the p21^{WAF1} structure is similar to that of p27^{KIP1}. Indeed, limited proteolysis, CD and NMR analyses have previously shown p21^{WAF1} to be unstructured in solution, as is p27^{KIP1} (Kriwacki *et al.*, 1996).

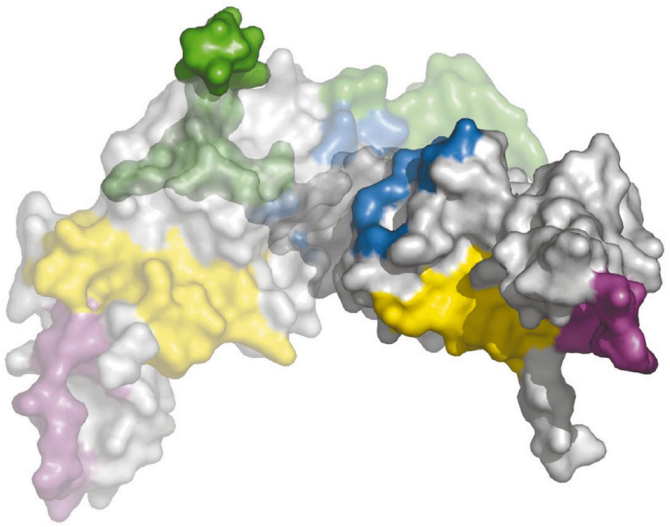

Figure 7
Interacting regions reported in different studies: N-terminal region (in yellow; Götz *et al.*, 2000; Romero-Oliva & Allende, 2001), acidic loop (magenta; Götz *et al.*, 2000), far C-terminal region (green; Götz *et al.*, 2000) and dimerization region (blue, this work). One of the protomers is represented semi-transparently in order to show the intertwined C-terminal regions in CK2 dimer. The structure represented is 1jwh in order to include the C-terminal region (Niefind *et al.*, 2001).

(ii) The different interacting regions mentioned in p21^{WAF1}-binding assays to CK2β (Götz *et al.*, 1998, 2000; Romero-Oliva & Allende, 2001) lie in a continuous band at the surface of the CK2β structure (Fig. 7).

(iii) It has been previously reported that p21^{WAF1} probably binds both catalytic and regulatory subunits of CK2 (Götz *et al.*, 1998).

(iv) The crystal structure of CK2β showed that an extended linear ridge of conserved residues is wrapped around the dimer structure (Chantalat *et al.*, 1999).

The conserved polybasic C-terminal region of p21^{WAF1}, not included in our peptide, most probably interacts with the acidic loop of CK2β (Leroy, Filhol *et al.*, 1997; Götz *et al.*, 2000), which is at the distal extremity of the previously mentioned interacting band. The interaction of this region of CK2β with wild-type p21^{WAF1} was demonstrated by Far-Western blot and pull-down assays (Romero-Oliva & Allende, 2001; Götz *et al.*, 2000). Additional potential binding sites may include the far C-terminal region of CK2β (201–215) (Romero-Oliva & Allende, 2001; Götz *et al.*, 2000).

The study of interactions of p21^{WAF1} with CK2β using small peptide fragments may not be an effective way of identifying all binding sites of the full-length p21^{WAF1}. It is clear that weak interactions in individual regions may act cooperatively to give tight binding to the CK2 holoenzyme. This could partly explain the discrepancies among several binding studies of p21^{WAF1} to CK2β (Götz *et al.*, 1998, 2000; Romero-Oliva & Allende, 2001).

We are grateful to Dr Graham Knight for the synthesis of the p21^{WAF1} fragment, Dr Richard Turner for the MALDI–TOF analysis and Florian Schmitzberger and Dr Dima Chirgadze for their structural advice (Department of Biochemistry, University of Cambridge). We wish to thank all the staff at beamline 14-1 at the ESRF and Dr Gunter Grossman at the SRS Daresbury for his contribution to SAXS data collection. This work was supported by the Wellcome Trust (GR046073 to TLB, GR064911 to JEA and WT062044 to VMB-G). LB acknowledges the financial support of the École Polytechnique and the Royal Society.

References

Allende, J. E. & Allende, C. C. (1995). *FASEB J.* **9**, 313–323.
Appel, K., Wagner, P., Boldyreff, B., Issinger, O. G. & Montenarh, M. (1995). *Oncogene*, **11**, 1971–1978.
Boldyreff, B., Meggio, F., Pinna, L. A. & Issinger, O. G. (1993). *Biochemistry*, **32**, 12672–12677.
Boldyreff, B., Meggio, F., Pinna, L. A. & Issinger, O. G. (1994*a*). *J. Biol. Chem.* **269**, 4827–4831.
Boldyreff, B., Meggio, F., Pinna, L. A. & Issinger, O. G. (1994*b*). *Cell. Mol. Biol. Res.* **40**, 391–399.
Brünger, A. T., Adams, P. D., Clore, G. M., DeLano, W. L., Gros, P., Grosse-Kunstleve, R. W., Jiang, J.-S., Kuszewski, J., Nilges, M., Pannu, N. S., Read, R. J., Rice, L. M., Simonson, T. & Warren, G. L. (1998). *Acta Cryst.* D**54**, 905–921.
Collaborative Computational Project, Number 4 (1994). *Acta Cryst.* D**50**, 760–763.

Chantalat, L., Leroy, D., Filhol, O., Nueda, A., Benitez, M. J., Chambaz, E. M., Cochet, C. & Dideberg, O. (1999). *EMBO J.* **18**, 2930–2940.
Chen, I. T., Akamatsu, M., Smith, M. L., Lung, F. D., Duba, D., Roller, P. P., Fornace, A. J. & O'Connor, P. M. (1996). *Oncogene*, **12**, 595–607.
DeLano, W. L. (2002). *The PyMOL Molecular Graphics System.* San Carlos, CA, USA: DeLano Scientific.
Flaugh, S. L. & Lumb, K. J. (2001). *Biomacromolecules*, **2**, 538–540.
Glover, C. V. C. (1986). *J. Biol. Chem.* **261**, 14349–14354.
Götz, C., Kartarius, S., Scholtes, P. & Montenarh, M. (1998). *Cancer Mol. Biol.* **5**, 1189–1205.
Götz, C., Kartarius, S., Scholtes, P. & Montenarh, M. (2000). *Biochem. Biophys. Res. Commun.* **268**, 882–885.
Götz, C., Wagner, P., Issinger, O. G. & Montenarh, M. (1996). *Oncogene*, **13**, 391–398.
Guerra, B. & Issinger, O. G. (1999). *Electrophoresis*, **20**, 391–408.
Hinrichs, M. V., Gatica, M., Allende, C. C. & Allende, J. E. (1995). *FEBS Lett.* **368**, 211–214.
Holland, P. M. & Cooper, J. A. (1999). *Curr. Biol.* **9**, 329–331.
Kabsch, W. & Sander, C. (1983). *Biopolymers*, **22**, 2577–2637.
Kleywegt, G. J. (1996). *Acta Cryst.* D**52**, 842–857.
Kriwacki, R. W., Hengst, L., Tennant, L., Reed, S. & Wright, P. E. (1996). *Proc. Natl Acad. Sci. USA*, **93**, 11504–11509.
Leroy, D., Filhol, O., Delcros, J. G., Pares, S., Chambaz, E. M. & Cochet, C. (1997). *Biochemistry*, **36**, 1242–1250.
Leroy, D., Heriche, J. K., Filhol, O., Chambaz, E. M. & Cochet, C. (1997). *J. Biol. Chem.* **272**, 20820–20827.
Leslie, A. (1992). *Jnt CCP4/ESF–EAMCB Newsl. Protein Crystallogr.* **26**.
Litchfield, D. W. (2003). *Biochem. J.* **369**, 1–15.
Meggio, F., Boldyreff, B., Issinger, O. G. & Pinna, L. A. (1994). *Biochemistry*, **33**, 4336–4342.
Meggio, F. & Pinna, L. A. (2003). *FASEB J.* **17**, 349–368.
Niefind, K., Guerra, B., Ermakowa, I. & Issinger, O. G. (2001). *EMBO J.* **20**, 5320–5331.
Niefind, K., Guerra, B., Pinna, L. A., Issinger, O. G. & Schomburg, D. (1998). *EMBO J.* **17**, 2451–2462.
Pearson, W. R. & Lipman, D. J. (1988). *Proc. Natl Acad. Sci. USA*, **85**, 2444–2448.
Pinna, L. A. & Meggio, F. (1997). *Prog. Cell Cycle Res.* **3**, 77–97.
Qian, X., Gozani, S., Yoon, H., Jeon, C., Agarwal, K. & Weiss, M. (1993). *Biochemistry*, **32**, 9944–9959.
Rekha, N. & Srinivasan, N. (2003). *BMC Struct. Biol.* **3**, 4.
Romero-Oliva, F. & Allende, J. E. (2001). *J. Cell Biochem.* **81**, 445–452.
Rost, B. & Sander, C. (1993). *Proc. Natl Acad. Sci. USA*, **90**, 7558–7562.
Russo, A. A., Jeffrey, P. D., Patten, A. K., Massagué, J. & Pavletich, N. P. (1996). *Nature (London)*, **382**, 325–331.
Svergun, D. I. (1991). *J. Appl. Cryst.* **24**, 485–492.
Tapia, J. C., Bolanos-Garcia, V. M., Sayed, M., Allende, C. C. & Allende, J. E. (2004). *J. Cell Biochem.* **91**, 865–879.
Thompson, J. D., Gibson, T. J., Plewniak, F., Jeanmougin, F. & Higgins, D. G. (1997). *Nucleic Acids Res.* **24**, 4876–4882.
Valero, E., De Bonis, S., Filhol, O., Wade, R. H., Langowski, J., Chambaz, E. M. & Cochet, C. (1995). *J. Biol. Chem.* **270**, 8345–8452.